Journal of Cell Science 104, 917-927 (1993)
Printed in Great Britain © The Company of Biologists Limited 1993

The regulation of bidirectional mitochondrial transport is coordinated with axonal outgrowth

Robert L. Morris* and Peter J. Hollenbeck*,†

Department of Anatomy and Cellular Biology, and Program in Cell and Developmental Biology, Harvard Medical School, 220 Longwood Ave, Boston, MA 02115, USA

*Present address: Department of Neurobiology, Harvard Medical School, 220 Longwood Avenue, Boston, MA 02115, USA
†Author for correspondence

SUMMARY

Although small molecules such as ATP diffuse freely in the cytosol, many types of cells nonetheless position their mitochondria in regions of intense ATP consumption. We reasoned that in the highly elongated axonal processes of growing neurons in culture, the active growth cone would form a focus of ATP consumption so distant from the cell body as to require the positioning of mitochondria nearby via regulated axonal transport. To test this hypothesis, we quantified the distribution and transport behavior of mitochondria in live, aerobically respiring chick sympathetic neurons. We found that in the distal region of actively growing axons, the distribution of mitochondria was highly skewed toward the growth cone, with a sevenfold higher density in the region immediately adjacent to the growth cone than in the region 100 μm away. When axonal outgrowth was blocked by substratum-associated barriers or mild cytochalasin E treatment, the gradient of mitochondrial distribution collapsed as mitochondria exited retrogradely from the distal region, becoming uniformly distributed along the axon within one hour. Analysis of individual mitochondrial behaviors revealed that mitochondrial movement everywhere was bidirectional but balanced so that net transport was anterograde in growing axons and retrograde in blocked axons. This reversal in net transport derived from two separate modulations of mitochondrial movement. First, moving mitochondria underwent a transition to a persistently stationary state in the region of active growth cones that was reversed when growth cone activity was halted. Second, the fraction of time that mitochondria spent moving anterogradely was sharply reduced in non-growing axons. Together, these could account for the formation of gradients of mitochondria in growing axons and their dissipation when outgrowth was blocked. This regulated transport behavior was not dependent upon the ability of mitochondria to produce ATP. Our data indicate that mitochondria possess distinct motor activities for both directions of movement and that mitochondrial transport in axons is regulated by both recruitment between stationary and moving states, and direct regulation of the anterograde motor.

Key words: axonal transport, mitochondria, organelle motility

INTRODUCTION

The functional asymmetry of eucaryotic cells gives rise to different requirements for macromolecules and energy in different regions of the cell. To address these needs, cells have evolved complex and tightly controlled mechanisms to transport and position different organelles in specific regions of the cytoplasm (e.g. see Ho et al., 1989; Hollenbeck and Swanson, 1990; Lee et al., 1989; Corthésy-Theulaz et al., 1992). The elaboration of organelle transport to support cellular asymmetry reaches its zenith in neurons, whose long axonal processes lack synthetic capacity and are supported by the copious bidirectional traffic of organelles between the cell body and terminal region (reviewed by Grafstein and Forman, 1980). Axonal organelle transport seems likely to be driven entirely or in part, by the microtubule-based motor proteins kinesin and cytoplasmic dynein (Vale et al., 1985a; Paschal et al., 1987), which generate movement in opposite directions along the axon's polarized microtubule array (Burton and Paige, 1981; Heidemann et al., 1981). However, despite extensive studies of the biochemical and biophysical characteristics of the proteins that drive movement, the mechanisms by which transport is regulated to appropriately position specific classes of organelles are essentially unknown. In fact, with one exception (Hollenbeck and Bray, 1987), we lack information about how the movement of any particular class of neuronal organelle is modulated in response to normal physiological changes.

In this study, we have examined the regulation of mitochondrial movement in the axons of peripheral neurons grown in culture. Since ATP is a small molecule and there-

fore freely diffusible in the cell, the specific location of mitochondria within the cell might in principle seem to be unimportant, and one might wonder why their transport should be regulated at all. However, it has been clear for some time that many cell types, such as epithelia, do position their mitochondria in regions of intense ATP consumption (Fawcett, 1981; Zielinski et al., 1988; Van Blerkom, 1991), indicating that even cells of relatively modest dimensions do not rely entirely on diffusion to ensure adequate delivery of ATP to ion pumps and other ATPases. In the highly elongated axonal processes of growing peripheral neurons, the active growth cone provides a region of intense ATP consumption so distant from the cell body that it could require the positioning of mitochondria nearby via regulated axonal transport. To test this hypothesis, we observed and quantified the distribution and transport behavior of mitochondria in both growing and non-growing axons, under aerobic and anaerobic conditions. Because axonal mitochondria are both easily recognizable and constrained to move in simple linear paths by the small diameter of the axon, they provide an ideal subject for quantitative studies of the regulation of motility. Our data reveal that mitochondrial transport in the distal axon is regulated in concert with the growing state of the axon but independent of mitochondrial ATP-generating capacity.

MATERIALS AND METHODS

Materials

All tissue culture media and supplements, and cytochalasin E, were obtained from Sigma Chemical Co. (St. Louis, MO). 4-(4-diethylaminostyryl)-*N*-methylpyridinium (4-di-2-ASP) and rhodamine 123 were obtained from Molecular Probes, Inc. (Eugene, OR). Texas Red-conjugated donkey anti-rabbit IgG was obtained from Vector Labs (Burlingame, CA). Anti-cytochrome *c* oxidase polyclonal antibody was a gift from A. Miranda. Ruled coverslip masks were prepared by Agar Scientific (Cambridge, UK).

Cell culture

Sympathetic chain ganglia were dissected from 9- to 11-day-old chicken embryos and cultured as whole ganglia or dissociated and grown as single cells on coverslips as previously described (Hollenbeck et al., 1985). Cells were grown for 18-26 h in a humidified 37˚C incubator in Liebovitz L-15 medium supplemented with 10% fetal bovine serum, 0.6% glucose, 2 mM L-glutamine, 100 i.u./ml penicillin, 100 μg/ml streptomycin, 50 ng/ml nerve growth factor, and 0.5% methyl cellulose. Coverslips were treated with 1 mg/ml polylysine followed by a laminin-enriched fraction of conditioned medium (prepared as per Lander et al., 1982) for 20-60 min each before plating out cells. Live cells were observed using a Zeiss IM35 or Axiophot microscope, and cultures were maintained at 37˚C with an air curtain stage-warmer.

For studies of mitochondrial transport in non-growing axons, elongation was blocked by either a substratum-associated barrier or mild drug treatment as previously described (Hollenbeck and Bray, 1987). Briefly, substratum-associated barriers were produced by shadowing silicon monoxide through a metallic electroformed mask to create 7 μm wide × 50-800 μm long adherent tracks on silane-treated coverslips. After a brief treatment of the coverslips with laminin, sympathetic neurons were plated onto them at low density. During subsequent growth, axons extended only to the ends of the tracks where their elongation was blocked by the surrounding siliconized surface. In other experiments, a low dose of cytochalasin E (1 μg/ml) was administered to cells to halt outgrowth rapidly.

To grow cells under anaerobic conditions, cultures were maintained as usual for 16 h, then the culture medium was withdrawn and replaced with a 1 mm-deep layer of medium containing 10 mM HEPES but lacking methyl cellulose. Culture dishes were sealed in a BBL GasPak Pouch (Becton Dickinson Microbiology Systems, Cockeysville, MD) for 4-24 h. Cells were fixed immediately after removal from the GasPak.

Measurements of mitochondrial distribution

For analyses of mitochondrial distribution and motility, unbranched axons of uniform caliber with distinct growth cones were selected, and measurements were made in the most distal 100 μm of each axon. Morphometry was performed using either BioRad MRC 600 software or an Image-1 Image Analysis System (Universal Imaging Corp., West Chester, PA). In live aerobic cells, mitochondria were stained with either 4-di-2-ASP (20 μM for 10 min) or rhodamine 123 (0.1 μg/ml for 30 min) and their distributions were measured by one of three techniques: (1) positions of individual mitochondria were revealed by epifluorescent illumination and quantified by measuring the distance from the base of the growth cone to the center point of each axonal mitochondrion. (2) To determine the distribution of mitochondrial length in the axons, epifluorescent images of neurons were gathered using a BioRad MRC 600 confocal laser scanner mounted on a Zeiss Axiophot microscope. The confocal apertures were opened wide enough to allow the fluorescence from the entire thickness of the axon to be collected. The distance from the base of the growth cone to the proximal and distal tips of each mitochondrion were measured, and the data were compiled as the total mitochondrial length in each of ten 10 μm bins comprising the distal 100 μm of axon. (3) The distribution of mitochondrial electrochemical potential was determined in rhodamine 123-labeled axons by using the confocal microscope and image analysis software to quantify the fluorescence intensity in consecutive 5 μm segments of axon and in equivalently sized areas of laterally adjacent background for the 100 μm of axon proximal to the growth cone. After subtracting corresponding background values for each segment, adjacent 5 μm segments were paired and summed to produce total mitochondrial fluorescence intensities for ten 10 μm bins. Mitochondria within the growth cones themselves could not be accurately quantified due to the wide variation in growth cone dimensions, which makes measurements of mitochondrial density per unit length of axon meaningless there.

To determine whether mitochondrial distributions departed significantly from uniform, data were analyzed statistically by linear regression with analysis of variance, chi-square and Kolmogorov-Smirnov tests for grouped data. Distributions are refered to as “skewed” if they differed significantly from a uniform distribution by all three tests at a significance level of $P < 0.01$. Distributions are refered to as “flat”, “even” or “level” if they were not significantly different from a uniform distribution by at least two of these three tests at $P < 0.05$.

The mitochondrial distribution in anaerobic cells was determined by immunofluorescent staining of cytochrome *c* oxidase. Cells were removed from an anaerobic GasPak, fixed immediately for 15 min at 37ºC, with 2.67% paraformaldehyde, 1.46% lysine, 0.23% sodium periodate, 0.73 mM $CaCl_2$ and 0.37 mM $MgCl_2$, in PBS, pH 7.4 (adapted from McLean and Nakane, 1974), permeabilized with 0.1% Triton X-100 in PBS, pH 7.4, and blocked with 3% BSA in PBS, pH 7.4. They were then incubated for 1 h in polyclonal anti-cytochrome *c* oxidase antibody diluted 1:300, washed, incubated for 1 h in Texas Red-conjugated goat

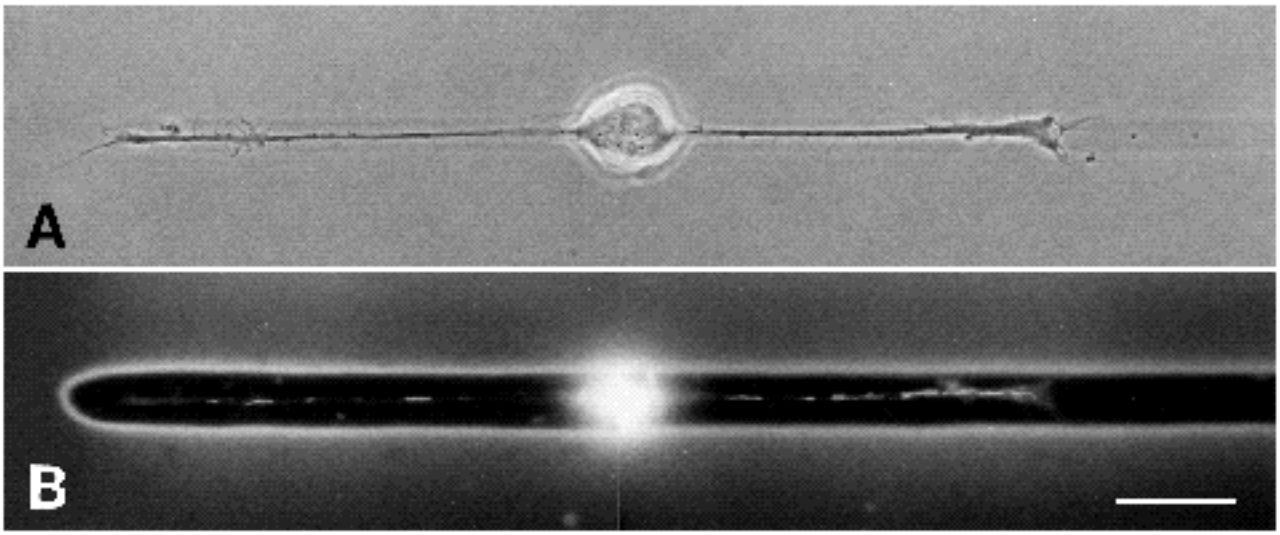

Fig. 1. A live sympathetic neuron labeled with the fluorescent vital dye 4-di-2-ASP growing on a shadowed adhesive strip on a siliconized coverslip. (A) Phase-contrast image showing a blocked axon on the left and an actively growing axon on the right. (B) Epifluorescent image showing the distribution of mitochondria. In this typical cell, the mitochondria in the growing axon are more numerous than in the non-growing axon and are distributed preferentially toward the advancing growth cone. Bar, 25 μm.

anti-rabbit IgG diluted 1:1000, washed and mounted with 1 mg/ml phenylenediamine in 90% glycerol/10% 10 × PBS (Johnson and Nogueira Araujo, 1981). Labeled cells were viewed on the scanning confocal microscope and the distribution of mitochondrial length was quantified as described in technique (2), above.

Measurement of mitochondrial movements and velocities

The movements of mitochondria were quantified in two discrete regions of growing and non-growing axons: (1) between 0 and 40 μm from the base of the growth cone and (2) between 60 and 100 μm from the base of the growth cone. This separation of regions eliminates possible confusion from behavior occurring on the border between observed zones. Axons were viewed by video-enhanced phase-contrast microscopy, using a Hamamatsu Newvicon camera, an Image-1 image analysis system to provide background subtraction and contrast enhancement, and a Panasonic AG-7300 Super-VHS video cassette recorder to record images. Videotaped movements of individual mitochondria were quantified with a Mark-V video measurement system (M. Walsh Electronics, San Dimas, CA) driven by Measure software (gift of Steven M. Block, Rowland Institute, Cambridge, MA). Based upon comparisons between phase-contrast and rhodamine 123 epifluorescence images, phase-dark organelles which were 0.5 μm across and at least 1 μm long were considered to be mitochondria. To prevent bias in selection of mitochondria for measurement, all mitochondria visible in the regions 0-40 μm and 60-100 μm from the growth cone over a 5 min period were tracked for the entire time they remained in focus. All mitochondrial displacement data for one region were then pooled. To correct for apparent movement of mitochondria due to drift of the stage, noise in the tracking system, etc., a threshold velocity of 0.05 μm/s was selected for two reasons: this was the average velocity of mitochondrial movements identified qualitatively as drift during recording, and was also equal to the value of the distance error in mouse positioning divided by the average duration of one measurement. Velocities below this "drift" velocity were considered to be zero. "Maximum" velocities were calculated from any movements which were sudden, clearly visible and of uniform velocity for their entire duration.

RESULTS

Analysis of mitochondrial distribution in growing and halted axons

To ascertain whether the growth state of the axon had any effect on the transport and positioning of its mitochondria, we compared the mitochondrial distributions of growing and non-growing axons from the same cell body. Plating chick embryonic sympathetic neurons onto coverslips containing defined adherent tracks (as described in Materials and methods) constrained the pattern of their outgrowth to the production of either a single axon or two axons growing at 180° from each other, from opposite sides of the cell body. When a growth cone arrived at the end of a track, its continued outgrowth was blocked by the non-adhesive siliconized surface of the coverslip; in cases where one axon of a bipolar neuron was halted while the other continued to elongate, the distribution of mitochondria in a growing and a non-growing axon from the same cell could be compared. Mitochondrial 4-di-2-ASP staining in these neurons revealed a striking difference between actively elongating and blocked axons: in elongating axons, the mitochondrial distribution appeared to form a gradient with the highest density near the growth cone, while blocked axons had lost this gradient and also had fewer mitochondria overall (Fig. 1).

To quantify these observations, we used the lipophilic cationic dyes 4-di-2-ASP (Magrassi et al., 1987) and rhodamine 123 (Johnson et al., 1981) to reveal the positions of mitochondria in live cells, and we halted outgrowth with a low dose of cytochalasin E (Cooper, 1987; Hollenbeck and Bray, 1987), so that the time at which growth cone activity ceased could be known with some accuracy for a large population of axons. 4-di-2-ASP reveals the position and dimensions of the mitochondria, while the fluorescence intensity of rhodamine 123 reports the magnitude of mito-

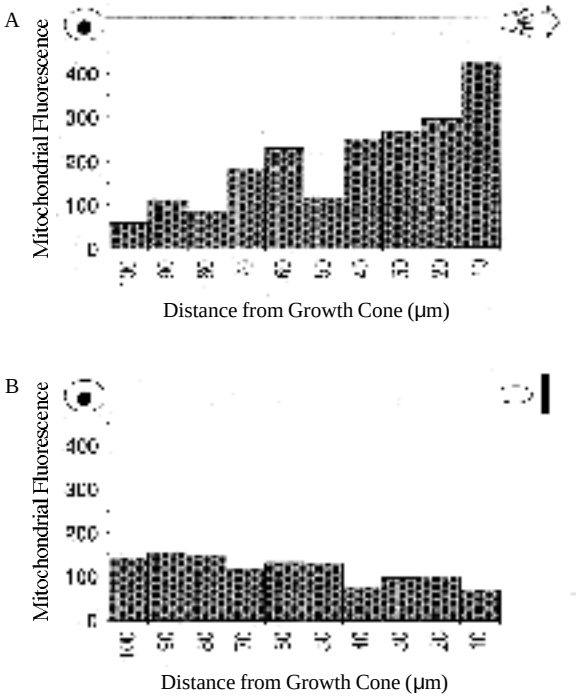

Fig. 2. Histograms of the intensity of mitochondrial rhodamine 123 fluorescence vs distance from the growth cone in the distal 100 μm of axons in aerobic cultures. Rhodamine 123 fluorescence intensity indicates the magnitude of mitochondrial membrane potential, which is related to the oxidative phosphorylation capacity of the mitochondrion. (A) The fluorescence distribution in actively elongating axons shows that mitochondrial ATP-generating capacity is highly skewed toward the growth cone. (B) The fluorescence distribution in the axons became uniform after growth had been blocked for 1 h by cytochalasin treatment, and the total ATP-generating capacity in the distal 100 μm (represented by the area under the whole histogram) dropped to 57% of the original value. The relative distributions were derived from quantifying rhodamine 123 fluorescence, but since the units of fluorescence are arbitrary, the total areas under the bars for growing and blocked axons were scaled on the basis of measurements of total mitochondrial length in the distal 100 μm of the same axons used for the fluorescence measurements. Data are derived from analysis of approximately 250 mitochondria in 12 growing axons, and approximately 440 mitochondria in 12 non-growing axons.

chondrial transmembrane potential as well (Johnson et al., 1981), and thus indicates not just the physical distribution of mitochondria, but the distribution of oxidative phosphorylation capacity. When we quantified the rhodamine 123 fluorescence intensity in the 100 μm of axon adjacent to active growth cones, we found a significantly skewed distribution, with a sevenfold higher density of mitochondrial fluorescence near the growth cone than at a distance of 100 μm away (Fig. 2A). When axonal elongation was halted, this distribution gradient disappeared as the mitochondria became redistributed away from the growth cone, assuming a statistically flat, uniform distribution within 1 h (Fig. 2B). Furthermore, the total mitochondrial length in the entire distal 100 μm of the axon, as represented by the area under the distribution histograms, became substantially reduced, indicating that mitochondria were leaving the distal axon entirely. This growth-dependent gradient of mitochondrial distribution, and its dissipation when growth was halted, were also seen when the distribution was quantified with 4-di-2-ASP in terms of physical length of mitochondria per unit length of axon, or by simply plotting the positions of the midpoint of each mitochondrion regardless of its length (data not shown). In addition, similar quantitative results were obtained when outgrowth was halted by culturing cells on patterned substrata as described above (Fig. 1) rather than by drug treatment. All distributions were analyzed statistically for significant deviation from an even distribution as described in Materials and Methods. We saw no evidence of mitochondrial division in the axon.

Regulation of mitochondrial motility during the maintenance and breakdown of distribution gradients

In order to understand how mitochondrial movements were modulated to form the distribution gradient in growing axons and to disperse it in non-growing axons, we analyzed the motile behavior of individual mitochondria by video-enhanced phase-contrast microscopy. Mitochondria were tracked and their motile behavior was analyzed in two separate regions of the distal axon: "near" the growth cone (0-40 μm from the base of the growth cone) and "far" from the growth cone (60-100 μm from the base of the growth cone). Separating the distal 100 μm of axon into two non-overlapping zones eliminated possible confusion of classifying types of behavior occurring in the border region. The duration and distance of all mitochondrial movements or stationary periods were then measured both near to and far from the growth cone in growing and non-growing axons. To ensure that measurements were taken during the time that the distribution gradient was being dissipated, data were gathered within 20 min of blocking growth.

Although individual mitochondria throughout the distal axon displayed movement in both directions along with periods of quiescence (Fig. 3), calculation of the rates of net directional transport and of the motile duty cycle (percentage of time spent moving) for the entire population revealed both growth-dependent and position-dependent characteristics of mitochondrial movement (Table 1). First, anterograde and retrograde movements combined to produce net anterograde transport in growing axons and net retrograde transport in non-growing axons. Second, the rate of net anterograde movement in growing axons was highest when mitochondria were still far from the growth cone and slowed to near zero in the region near the growth cone. In non-growing axons, however, the rate of net retrograde movement was highest near the growth cone and decreased somewhat when mitochondria were farther away. These modulations of net transport would clearly serve to deliver mitochondria to an active growth cone, and to reverse the process when growth cone advance ceased.

The duty cycle of the mitochondria revealed a striking pattern as well: the majority of the mitochondria's time in the axons was spent stationary (Table 2). Because of this widely imbalanced duty cycle, we analyzed the moving mitochondria separately from the persistently stationary ones in order to reveal more about the underlying mecha-

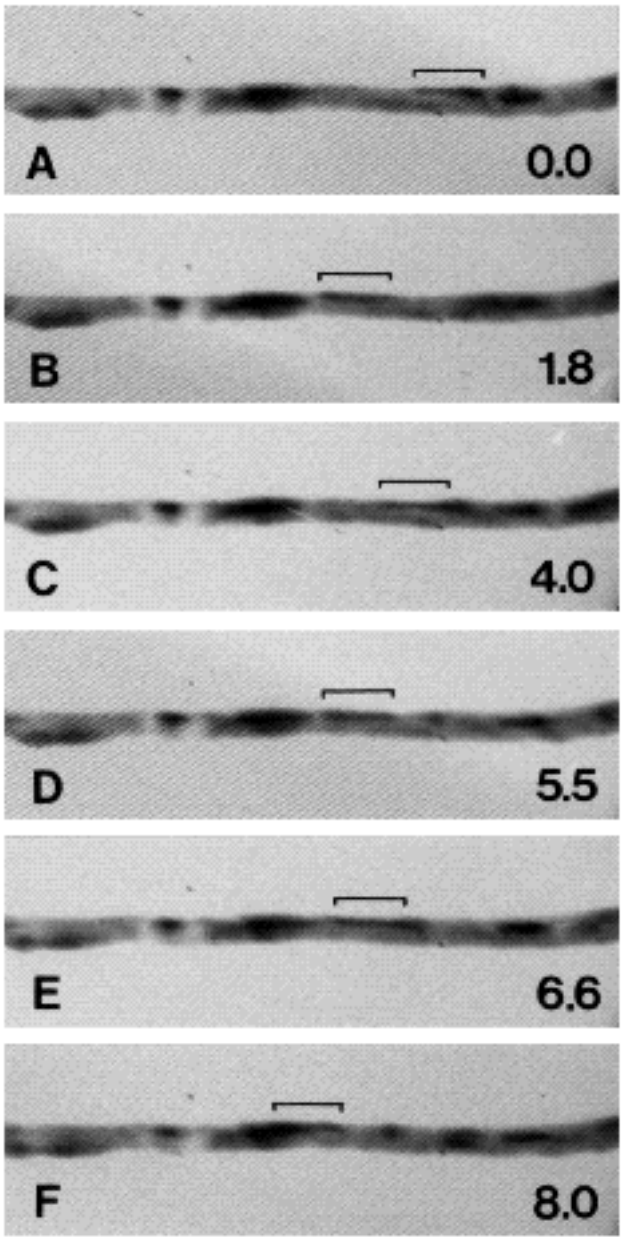

Fig. 3. An example of bidirectional transport of a mitochondrion in an axon growing under aerobic conditions. With the growth cone out of view to the right, this typical series of video frames shows a mitochondrion (marked by bracket) moving retrogradely (A to B), then anterogradely (B to C), then retrogradely (C to D), then slightly anterogradely (D to E), then retrogradely (E to F). The 2 μm long mitochondrion begins in frame A at 60 μm from the active growth cone and undergoes a net retrograde displacement of 5 μm in this sequence. Although this sequence is taken far from the growth cone in a growing cell, all regions of growing and non-growing axons showed similar mitochondrial behavior and maximal velocities. Elapsed time is shown in seconds at the lower right of each frame. The image frames show the same 20 μm segment of axon.

nisms regulating the net transport. A mitochondrion was classified as "moving" if it showed significant motion during the observation time as judged by one of two criteria: (1) achieving a velocity at any time during tracking that met or exceeded the slowest "maximum" velocity measured in that direction; (2) displaying persistent movement that achieved a net velocity over the entire time it was observed of 0.05 μm/s. "Maximum" velocities and the choice of this threshold velocity are explained in Materials and Methods.

When these criteria were applied to all mitochondria in growing and non-growing axons, three patterns emerged (Table 2). First, in growing axons, there was a large regional difference in duty cycle. Only 25% of the mitochondria near the growth cone moved significantly during observation, with the other 75% remaining stationary, while far from the growth cone the inverse was the case, with 75% of the mitochondria moving and only 25% remaining stationary. Second, blocking axonal growth significantly increased the percentage of moving mitochondria. Near the blocked growth cones almost 60% of the mitochondria moved, as

Table 1. Duty cycles (percentage of time moving one direction) and net displacements of the entire mitochondrial population in growing and non-growing axons

	% of time	Mean velocity (μm/s)	Total displacement per 100 s (μm)
Growing cells			
Near growth cone			
Anterograde movement	11	0.24	2.69
Retrograde movement	7	−0.33	−2.15
Stationary	82	0.00	0.00
			Net = 0.55
Far from growth cone			
Anterograde movement	15	0.42	6.57
Retrograde movement	10	−0.41	−4.13
Stationary	74	0.00	0.00
			Net = 2.44
Non-growing cells			
Near growth cone			
Anterograde movement	5	0.24	1.08
Retrograde movement	9	−0.56	−4.84
Stationary	87	0.00	0.00
			Net = −3.76
Far from growth cone			
Anterograde movement	7	0.32	2.27
Retrograde movement	6	−0.69	−4.35
Stationary	87	0.00	0.00
			Net = −2.08

Near growth cone, the region 0-40 μm from the base of the growth cone. Far from growth cone, the region 60-100 μm from the base of the growth cone. Displacements and velocities in the anterograde direction are recorded as positive and in the retrograde direction as negative. All mitochondrial displacement data for growing or non-growing cells, near or far from growth cone, were pooled and % of time column is calculated from these pools. Mean velocity was calculated by dividing the total anterograde or retrograde distance of movement by the total time spent moving either anterogradely or retrogradely. Total displacement in the anterograde or retrograde direction was determined by multiplying % of time moving in one direction by the mean velocity in that direction. Net displacement is the sum of total displacements. Data are derived from analysis of 48 mitochondria from 3 cells observed for 2956 s in growing axons near the growth cone; 24 mitochondria from 3 cells observed for 1832 s in growing axons far from the growth cone; 22 mitochondria from 3 cells observed for 4160 s in non-growing axons near the growth cone; 20 mitochondria from 3 cells observed for 3056 s in non-growing axons far from the growth cone.

Table 2. Mitochondria divided into moving or stationary populations in growing and non-growing cells

	Growing cells (% of mitoch.)	Non-growing cells (% of mitoch.)
Near growth cone		
Stationary	75	41
Moving	25	59
Moving only anterograde	10	5
Move only retrograde	10	9
Move both ant. and ret.	5	45
Far from growth cone		
Stationary	25	15
Moving	75	85
Moving only anterograde	8	0
Moving only retrograde	29	25
Move both ant. and ret.	38	60

Mitochondria were categorized as either moving or stationary, based on two selection criteria. Mitochondria were categorized as moving if they *either* achieved a velocity exceeding the slowest recorded maximal velocity (0.72 μm/s anterograde, −0.59 μm/s retrograde (see legend to Table 3) *or* achieved a net transport of > 0.05 μm/s over the entire time they were observed. Mitochondria which did not meet either of these criteria were designated stationary as they exhibited neither rapid nor persistent movements. All mitochondria analyzed in Table 1 were classified in this way and included here, therefore percentages of mitochondria designated stationary and moving total to 100%. The moving population of mitochondria was further subdivided by the directions in which they moved.

Table 3. Duty cycles and net displacements of moving mitochondria in growing and non-growing axons

	% of time	Mean velocity (μm/s)	Total displacement per 100 s (μm)	Mean maximum velocity (μm/s)
Growing cells				
Near growth cone				
Anterograde movement	33	0.26	8.66	1.58
Retrograde movement	12	−0.63	−7.74	−2.01
Stationary	55	0.00	0.00	0.00
			Net = 0.92	
Far from growth cone				
Anterograde movement	17	0.50	8.26	1.43
Retrograde movement	12	−0.44	−5.31	−1.80
Stationary	71	0.00	0.00	0.00
			Net = 2.95	
Non-growing cells				
Near growth cone				
Anterograde movement	6	0.29	1.70	1.62
Retrograde movement	11	−0.44	−4.82	−1.72
Stationary	83	0.00	0.00	0.00
			Net = −3.12	
Far from growth cone				
Anterograde movement	9	0.32	2.83	1.45
Retrograde movement	8	−0.72	−5.44	−1.90
Stationary	84	0.00	0.00	0.00
			Net = −2.60	

Near growth cone, the region 0-40 μm from base of growth cone. Far from growth cone, the region 60-100 μm from the base of the growth cone. Displacements and velocities in the anterograde direction are recorded as positive and in the retrograde direction are negative. The displacement data for all mitochondria classified as moving in Table 2 were segregated and analyzed here. Movements which were sudden, clearly visible and of uniform velocity for their entire duration were defined as maximum and were averaged to obtain mean maximum velocity values. Other calculations were performed as described in Table 1 legend. Moving mitochondria data are derived from 12 mitochondria from 3 cells observed for 641 s in growing axons near the growth cone; 18 mitochondria from 3 cells observed for 1379 s in growing axons far from the growth cone; 13 mitochondria from 3 cells observed for 2101 s in non-growing axons near the growth cone; 17 mitochondria from 3 cells observed for 2432 s in non-growing axons far from the growth cone.

opposed to 25% in growing cells, and far from the growth cone there was also a small rise in the percentage that were moving. Third, when axonal growth was blocked, the percentage of mitochondria that moved *only* anterogradely dropped both near and far from the growth cone, while the percentage moving exclusively in a retrograde direction remained virtually the same as in growing axons.

To address the regulation of mitochondrial movement separately from the balance between persistently moving and stationary states, we segregated and analyzed the data for moving mitochondria alone (Table 3). As with the total mitochondrial population, the moving mitochondria underwent net anterograde transport in growing axons and net retrograde transport in blocked axons. Also, even these mitochondria, which moved significantly at least some time during observation, spent the majority of their time stationary. But the fraction of time that they spent in motion changed in one significant way when axonal outgrowth was blocked: the fraction of time mitochondria spent moving in the anterograde direction dropped dramatically when growth stopped, from 33% to only 6% of their time near the growth cone and from 17% to 9% far from the growth cone. Meanwhile, the fraction of time mitochondria moved in the retrograde direction changed very little when growth stopped either near to or far from the growth cone.

The mitochondria in the moving pool occasionally underwent periods of rapid, persistent movement, which were measured and averaged separately ("maximum velocities", Table 3). There was some variation in the maximum velocities of mitochondria, but the retrograde velocities were higher than the anterograde velocities. This is consistent with in vitro studies on the putative motor proteins for mitochondrial transport: kinesin driving anterograde transport (Vale et al., 1985a,b) and dynein driving retrograde transport (Paschal et al., 1987; Schnapp and Reese, 1989).

Mitochondrial distribution in anaerobically growing neurons

Finally, we asked the question of whether the regulation of mitochondrial distribution and motility was coupled to their normal function - the production of ATP by oxidative phosphorylation. To do this, we grew neurons under anaerobic conditions for 8-24 h in order to inhibit oxidative phosphorylation, then fixed them and determined the distribution of mitochondria in the distal axons by anti-cytochrome *c* immunofluorescence (Kuhn-Nentwig and Kadenbach, 1985). In cultures grown anaerobically for 8 h, the mitochondrial distribution in actively growing axons was skewed toward the growth cone (Fig. 4A), in a manner similar to that seen in aerobically grown cultures, with a twofold gradient between the region immediately adjacent to the growth cone and the region 100 μm away. When axonal outgrowth was blocked in these cultures, the mitochondria underwent a retrograde redistribution (Fig. 4B). In cultures maintained under anaerobic conditions for 24 h,

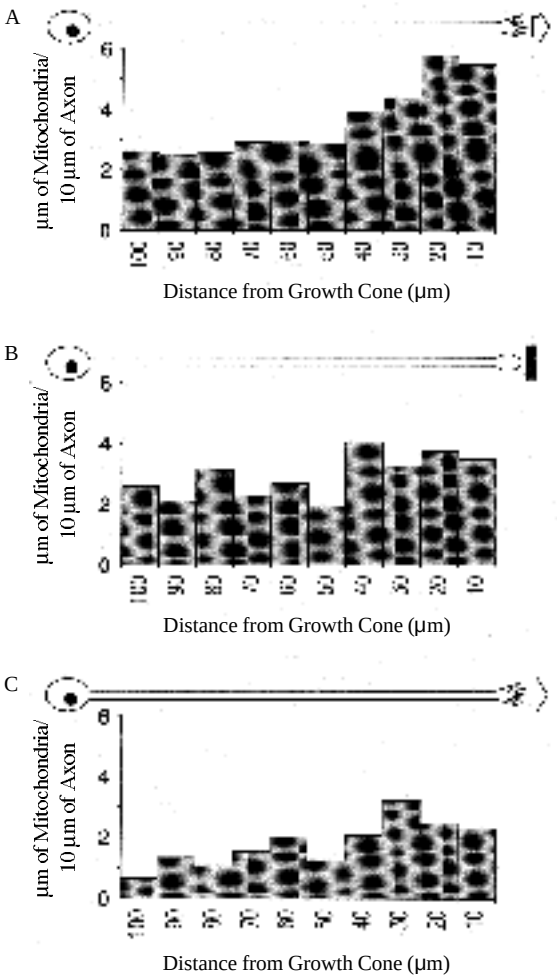

Fig. 4. Histograms of the density of mitochondria in the axon vs distance from the growth cone in the distal 100 µm of axons in cultures grown under anaerobic conditions. Mitochondria were detected by indirect immunofluorescence with a polyclonal anti-cytochrome *c* oxidase antibody and distributions were determined as described in Materials and Methods.
(A) Immunofluorescence distribution in actively elongating axons growing under anaerobic conditions for 8 h prior to fixation. Staining is significantly skewed toward the growth cone.
(B) Immunofluorescence distribution in axons grown under anaerobic conditions for 7 h then blocked for growth by cytochalasin treatment under anaerobic conditions for 1 h more prior to fixation and staining. The distribution has become flat, and the total fluorescence in the distal 100 µm (represented by the area under the whole histogram) has dropped to 82% of the value in aerobic cultures. (C) Immunofluorescence distribution in axons grown under anaerobic conditions for 24 h prior to fixation and staining is also skewed, but now the total fluorescence in the distal 100 µm has dropped to 60% of the value in the 8 h anaerobic cultures (Fig. 4A) and to 50% of the value in aerobic cultures (Fig. 2A). Data for (A) are derived from the lengths of 388 mitochondria in 21 cells, for (B) from 218 mitochondria in 14 cells, and for (C) from 116 mitochondria in 11 cells.

growing axons also showed a mitochondrial distribution that was skewed toward the growth cone, but this gradient had a smaller magnitude (Fig. 4C). In addition, the total mitochondrial density in the distal axons of these cells was 60% lower than in aerobically growing, and 50% lower than in 8 h anaerobically growing neurons.

DISCUSSION

Regulated motility creates or dissipates a skewed mitochondrial distribution

In this study, we have shown that the bidirectional axonal transport of mitochondria is regulated in concert with the growth state of the axon. In axons which were elongating, mitochondria were clustered into a steep gradient near the active growth cone, while in axons whose elongation was blocked, the mitochondria became evenly distributed. Because this behavior was observed whether we measured the distribution of mitochondrial number, mitochondrial length or mitochondrial rhodamine 123 fluorescence, it was clear that it represented regulated movement of mitochondria, and not just changes in their size or membrane potential in response to physiological changes in the axon.

While individual mitochondria moved bidirectionally (Fig. 3), tracking the average transport behavior of a large population of mitochondria confirmed that regional and growth-dependent regulation of their *net* transport created and dissipated the gradient (Table 1). In growing axons, the mitochondria moved in a net anterograde direction. When growth was blocked, mitochondrial transport rapidly shifted to net retrograde and the mitochondrial distribution gradient was quickly eliminated. Furthermore, the rate of net transport varied with their distance from the growth cone: in growing axons, net anterograde velocity was 4.4 times greater far from the growth cone than it was near the growth cone, while in halted axons the net retrograde velocity was 1.8 times greater near the growth cone than far away. Thus, the mitochondrial distribution gradient is established in growing axons by the relatively rapid approach of mitochondria to the distal region, followed by a reduction of their net anterograde velocity to roughly that of growth cone advance (Hughes, 1953). The dissipation of the gradient occurs by the relatively rapid exit of mitochondria from the growth cone region, followed by a slowing of the net retrograde velocity as mitochondria progress farther from the axon terminus. The result is a reduced density and a uniform distribution of mitochondria along the axon length rather than a complete evacuation of the distal region.

Mitochondrial motility is controlled at two levels

A detailed analysis of individual mitochondrial behavior (Tables 2 and 3) revealed that the net transport described above was generated by regulation at two levels. First, the transition between moving and stationary states was regulated along the length of growing axons to control the number of mitochondria which remained clustered near the growth cone in growing vs non-growing axons. Second, anterograde transport, but not retrograde transport, was selectively regulated between growth states to control the level and direction of net mitochondrial transport. By coordination of these two regulatory mechanisms, the skewed mitochondrial distributions were created and maintained in growing cells and eliminated when growth ceased.

The balance between moving and stationary pools of mitochondria

The number of mitochondria which exhibited significant movement varied considerably with distance from the growth cone and with the growth state of the axon. In growing axons, 75% of the mitochondria far from the growth cone were moving, but this fraction dropped by two-thirds as the mitochondria arrived near the growth cone. When growth was blocked, the moving mitochondrial fraction rose all along the axon, more than doubling near the growth cone and also rising far from the growth cone. These data are consistent with a conversion of mitochondria from a moving to a persistently stationary state in the distal region of growing axons, and a partial reversal of that process when axonal growth is halted.

The presence of a stationary pool of mitochondria has been suggested by evidence from both neuronal and non-neuronal cells, indicating apparent anchorage of mitochondria to stable elements in the axon. This includes morphological evidence showing attachment of mitochondria to the cell cortex (Forman et al., 1987; Lin et al., 1990) or the cytoskeleton, particularly the intermediate filaments (Hirokawa, 1982; Stromer and Bendayan, 1990), as well as some biochemical evidence suggesting stable associations with the cytoskeleton (Price and Gomer, 1989; Rendon et al., 1990; Leterrier et al., 1990). Such a stable attachment of the majority of mitochondria to the cytoskeleton upon arrival in the distal region of growing axons would explain both the maintenance of the distribution gradient seen there, and the "advance" of the stationary mitochondria at approximately the rate of growth cone advance (Hughes, 1953; Reinsch et al., 1991). It would also explain the reported codependence of mitochondrial distribution upon *both* the microtubule and intermediate filament systems (Summerhayes et al., 1983). The large increase in the moving pool of mitochondria when axonal outgrowth was halted could represent mitochondria freed from their anchorage to the "stationary" cytoskeleton, allowing modulation of their transport and subsequent redistribution.

Change in net direction is achieved via regulation of anterograde transport

The second level at which mitochondrial motility was controlled was the specific regulation of anterograde movement. This became apparent first when looking at the percentage of the whole mitochondrial population which moved exclusively anterogradely or retrogradely (Table 2). Here, when axonal outgrowth stopped, the percentage of mitochondria moving exclusively anterogradely dropped while the percentage moving exclusively retrogradely remained virtually the same. Separate analysis of the persistently moving mitochondrial population gave a complementary result: when axonal outgrowth ceased, the percentage of time that mitochondria spent moving anterogradely dropped sharply while the percentage of time spent moving retrogradely remained the same or dropped only slightly (Table 3). These differences held both near to and far from the growth cone, and were sufficient to explain the differences in the net direction of mitochondrial transport in growing and non-growing axons. This suggests that formation of the steep mitochondrial gradient in growing axons, and its dissipation in non-growing axons, is achieved almost entirely by regulation of the anterograde motor activity alone. When growth is blocked, the anterograde motor activity is reduced, allowing the steady activity of the retrograde motors to exert more influence. We find no evidence that mitochondrial retrograde motor activity is significantly regulated.

Do individual mitochondria have motors for both directions of movement?

Three lines of evidence presented here argue that mitochondria bear motor activities for both the anterograde and retrograde directions of movement. First, mitochondria change direction frequently and rapidly (Fig. 3), seemingly too quickly for the exchange of one set of motors for another. Second, the duty cycle data in Tables 2 and 3 indicate that anterograde mitochondrial transport is regulated independently of retrograde transport. Third, mitochondria move with different maximum velocities in the anterograde and retrograde directions (Table 3). These maximum velocities seem more likely to be characteristic properties of the motors driving mitochondrial movement than are the slower average velocity values reported here or reported previously (Forman et al., 1987; Takenaka et al., 1990), since the slower average velocities reflect variations in resistance to organelle movement through the axoplasm. Ultrastructural studies (Heggeness et al., 1978; Tsukita and Ishikawa, 1980; Hirokawa, 1982; Schnapp and Reese, 1982; Miller and Lasek, 1985; Van Blerkom, 1991) and in vitro experiments (Brady et al., 1982; Martz et al., 1984) have strongly implicated microtubules as the transport filament for mitochondria, and current thinking favors the action of two distinct classes of motor proteins in the production of organelle movements (reviewed by Schroer and Sheetz, 1990; Vallee and Bloom, 1991): kinesins driving anterograde movement (Vale et al., 1985b; Porter et al., 1987; Saxton et al., 1988; Hirokawa et al., 1991), and dyneins driving retrograde movement (Schnapp and Reese, 1989; Schroer et al., 1989). The fact that the maximum retrograde velocities for mitochondria were higher than anterograde velocities is consistent with kinesin and dynein driving mitochondrial movements (Vale et al., 1985a,b; Paschal et al., 1987). If this is the case, then our data implicate the specific regulation of kinesin in the transition between net anterograde and retrograde mitochondrial transport. However, our data in no way rule out a role for novel classes of microtubule-based motor proteins (Cole et al., 1992; Sawin et al., 1992) or even actin-based motor proteins (Bradley and Satir, 1979; Brady et al., 1984; Kuznetsov et al., 1992) in mitochondrial motility. Although cytochalasin E can disrupt the actin cortex at high concentration, we administered a low dose to block axonal outgrowth by inhibiting actin polymerization in the growth cone, without compromising the actin cortex integrity.

Possible signals and effectors for the regulation of mitochondrial transport

The reversal of net mitochondrial transport from anterograde to retrograde when axonal outgrowth is blocked raises the question of which intracellular signals control that

switch. Studies performed on regenerating or ligated nerves have demonstrated the reversal of axonal transport direction (Bray et al., 1971; Frizzel et al., 1976; Bulger and Bisby, 1978; Smith, 1988), and some have implicated proteases (Sahenk and Lasek, 1988; Smith and Snyder, 1991) or acidification (Edmonds and Koenig, 1987; Sahenk and Brown, 1991) in the reversal process. But these experiments involved severe insult to the cells and reversal of organelles that may not otherwise move retrogradely, and therefore may not be relevant to mitochondria which routinely change direction. One report suggests that ADP could be the molecule which signals mitochondria to cease movements (Bereiter-Hahn and Vöth, 1983), which could explain the clustering of mitochondria in regions of high ATP demand. The unique ionic environment of the growth cone, which is thought to control its motility (Cohan et al., 1987; Lankford et al, 1988; Mattson et al., 1988; Lankford and Letourneau, 1991; Rehder and Kater, 1992), may also play a role in controlling mitochondrial transport, which, as shown here, is dependent upon axonal outgrowth and is specifically regulated in the growth cone region. These intracellular signals may act through local modification of the phosphorylation state of the mitochondrial motor proteins or their putative receptors. Kinesin, the kinesin-associated protein kinectin and dynein are all phosphoproteins (Sato-Yoshitake et al., 1991; Farshori and Goode, 1991; Toyoshima et al., 1992; Chilcote and Johnson, 1990; Hamasaki et al., 1991; Hollenbeck, 1993), and may affect the motor activity (Chilcote and Johnson, 1990; Hamasaki et al., 1991) or the affinity of motor proteins for their receptors (Sato-Yoshitake et al., 1991; Farshori and Goode, 1991). Phosphorylation could serve to regulate the transition between the moving and stationary states in the growth cone region by acting at any of these levels. At least one kinase localizes to growth cones (Maness et al., 1988), and others may as well.

Does the regulation of mitochondrial transport depend upon whether or not the mitochondria are producing ATP? A guiding assumption in this study is that the reason mitochondrial distribution and transport are regulated at all in many cell types is to ensure adequate ATP levels at foci of intense energy consumption. An interesting question then was whether the regulated transport of mitochondria in axons was a “default” process, or whether it depended upon their capacity to supply ATP to the cytosol. Experiments performed under anaerobic conditions showed that after 8 h of anaerobic culture, growing axons still displayed a mitochondrial distribution gradient although a shallower one than in aerobic cultures (Fig. 4A), and that blocking outgrowth in these cultures caused mitochondrial redistribution as it had in aerobic cultures (Fig. 4B). Since the mitochondria were redistributed here, this argues that the skewed distribution in the growing anaerobic culture was not simply due to the lack of sufficient ATP to power a redistribution. Growing cultures maintained under anaerobic conditions for 24 h (Fig. 4C) revealed that even though the overall density of mitochondria in the distal axon had dropped to one half of the aerobic value, the few mitochondria which remained were still maintained in a skewed distribution. The reduction in mitochondrial density was most likely due to breakdown of mitochondrial inner membranes (Luzikov et al., 1971, 1973) and subsequent loss of cytochrome *c* oxidase for oxidative phosphorylation and for immunofluorescence detection. Thus, the regulatory mechanisms which retain mitochondria near the growth cone of growing axons, and free them to move retrogradely in non-growing axons, are not strictly dependent on aerobic mitochondrial metabolism.

The authors thank Dr A. Miranda for the generous gift of antibodies against cytochrome *c* oxidase, and Drs P. C. Bridgman and L. B. Chen for critically reading the manuscript. This work was supported by a grant from the National Institutes of Health (NS27073) and a Basil O’Connor Starter Scholar Award from the March of Dimes Birth Defects Foundation.

REFERENCES

Bereiter-Hahn, J. and Vöth, M. (1983). Metabolic control of shape and structure of mitochondria in situ. *Biol.Cell*. **47,** 309-322.

Bradley, T. J. and Satir, P. (1979). Evidence of microfilament-associated mitochondrial movement. *J. Supramol. Struct.* **12,** 165-175.

Brady, S. T., Lasek, R. J. and Allen, R. D. (1982). Fast axonal transport in extruded axoplasm from squid giant axon. *Science* **218,**1129-1131.

Brady, S. T., Lasek, R. J. and Allen, R. D., Yin, H. L., and Stossel, T. P. (1984). Gelsolin inhibition of fast axonal transport indicates a requirement for actin microfilaments. *Nature* **310,** 56-58.

Bray, J. J., Kon, C. M. and Breckenridge, B. McL. (1971). Reversed polarity of rapid axonal transport in chicken motoneurons. *Brain Res.* **33,** 560-564.

Bulger, V. T. and Bisby, M. A. (1978). Reversal of axonal transport in regenerating nerves. *J. Nerochem.* **31,** 1411-1418.

Burton, P. R. and Paige, J. L. (1981). Polarity of axoplasmic microtubules in the olfactory nerve of the frog. *Proc. Nat. Acad. Sci. USA* **78,** 3269-3273.

Chilcote, T. J. and Johnson, K. A. (1990). Phosphorylation of Tetrahymena 22 S dynein. *J. Biol. Chem.* **265,** 17257-17266.

Cohan, C. S., Conner, J. A. and Kater, S. B. (1987). Electrically and chemically mediated increases in intracellular calcium in neuronal growth cones. *J. Neurosci.* **7,** 3588-3599.

Cole, D. G., Cande, W. Z., Baskin, R. J., Skoufias, D. A., Hogan, C. J. and Schloley, J. M. (1992). Isolation of sea urchin kinesin-related protein using peptide antibodies. *J. Cell Sci.* **101,** 291-301.

Cooper, J. A. (1987). Effects of cytochalasin and phalloidin on actin. *J. Cell Biol.* **105,** 1473-1478.

Corthésy-Theulaz, I., Pauloin, A. and Pfeffer, S. R. (1992). Cytoplasmic dynein participates in the centrosomal localization of the Golgi complex. *J. Cell Biol.* **118,** 1333-1345.

Edmonds, B. and Koenig, E. (1987). Powering of bulk transport (varicosities) and differential sensitivities of directional transport in growing axons. *Brain Res.* **406,** 288-293.

Farshori, P. Q. and Goode, D. (1991). Kinesin is phosphorylated during stimulation of insulin secretion and associates with secretory granules in HIT cells. *J. Cell Biol.* **115,** 390a (Abstr).

Fawcett, D. W. (1981). Mitochondria. In *The Cell,* pp. 410-484. Philadelphia: W.B. Saunders Co.

Forman, D. S., Lynch, K. J. and Smith, R. S. (1987). Organelle dynamics in lobster axons: anterograde, retrograde, and stationary mitochondria. *Brain Res.* **412,** 96-106.

Frizell, M., Mclean, W. G. and Sjöstrand, J. (1976). Retrograde axonal transport of rapidly migrating labelled proteins and glycoproteins in regenerating peripheral nerves. *J. Neurochem.* **27,** 191-196.

Grafstein, B. and Forman, D. S. (1980). Intracellular transport in neurons. *Physiol. Rev.* **60,** 1167-1283.

Hamasaki, T., Barkalow, K., Richmond, J. and Satir, P. (1991). cAMP-stimulated phosphorylation of an axonemal polypeptide that copurifies with a 22 S dynein arm regulates microtubule translocation velocity and swimming speed in Paramecium. *Proc. Nat. Acad. Sci. USA* **88,** 7918-7922.

Heidemann, S. R., Landers, J. M. and Hamborg, M. A. (1981). Polarity orientation of axonal microtubules. *J. Cell Biol.* **91,** 661-665.

Heggeness, M. H., Simon, M. and Singer, S. J. (1978). Association of mitochondria with microtubules in cultured cells. *Proc. Nat. Acad. Sci. USA.* **75,** 3863-3866.

Hirokawa, N. (1982). Cross-linker system between neurofilaments, microtubules, and membranous organelles in frog axons revealed by the quick-freeze, deep-etching method. *J. Cell Biol.* **94,** 129-142.

Hirokawa, N., Sato-Yoshitake, R., Kobayashi, N., Pfister, K. K., Bloom, G. S. and Brady, S. T. (1991). Kinesin associates with anterogradely transported membranous organelles in vivo. *J. Cell Biol.* **114,** 295-302.

Ho, W. C., Allen, V. J., Van Meer, G., Berger, E. G. and Kreis, T. E. (1989). Reclustering of scattered Golgi elements occurs along microtubules. Eur. *J. Cell Biol.* **48,** 250-263.

Hollenbeck, P. J. (1993). Phosphorylation of neuronal kinesin heavy and light chains *in vivo. J. Neurochem.* **60**, (in press).

Hollenbeck, P. J. and Bray, D. (1987). Rapidly transported oganelles containing membrane and cytoskeletal components: their relation to axonal growth. *J. Cell Biol.* **105,** 2827-2835.

Hollenbeck, P. J., Bray, D. and Adams, R. J. (1985). Effects of the uncoupling agents FCCP and CCCP on the saltatory movements of cytoplasmic organelles. *Cell Biol. Int. Rep.* **9,** 193-199.

Hollenbeck, P. J. and Swanson, J. A. (1990). Radial extension of macrophage tubular lysosomes supported by kinesin. *Nature* **346,** 864-866.

Hughes, A. (1953). The growth of embryonic neurites. *J. Anat.* **87,** 150-162.

Johnson, G. D. and Nogueira Araujo, G. M. de C. (1981). A simple method for reducing the fading of immunofluorescence during microscopy. *J. Immunol. Meth.* **43,** 349-350.

Johnson, L.V., Walsh, M. L. Bockus, B. J. and Chen, L. B. (1981). Monitoring of relative mitochondrial membrane potential in living cells by fluorescence microscopy. *J. Cell Biol.* **88,** 526-535.

Kuhn-Nentwig, L. and Kadenbach, B. (1985). Isolation and properties of cytochrome C oxidase from rat liver and quantitation of immunological differences between isozymes from various rat tissues with subunit-specific antisera. *Eur. J. Biochem.* **149**, 147-158.

Kuznetsov, S. A., Langford, G. M. and Weiss, D. G. (1992). Actin-dependent organelle movement in squid axoplasm. *Nature* **356,** 722-725.

Lander, A. D., Fujii, D.K., Gospodarowicz, D. and Reichardt, L. F. (1982). Characterization of a factor that promotes neurite outgrowth: evidence linking activity to a heparin sulfate proteoglycan. *J. Cell Biol.* **94,** 574-585.

Lankford, K. L., DeMello, F. G. and Klein, W. L. (1988). D_1-type dopamine receptors inhibit growth cone motility in cultured retina neurons: evidence that neurotransmitters act as morphogenic growth regulators in the developing central nervous system. *Proc. Nat. Acad. Sci. USA* **85,** 2839-2843.

Lankford, K. L. and Letourneau, P. C. (1991). Roles of actin filaments and three second-messenger systems in short-term regulation of chick dorsal root ganglion neurite outgrowth. *Cell Motil. Cytoskel.* **20,** 7-29.

Lee, C., Ferguson, M. and Chen, L. B. (1989). Construction of the endoplasmic reticulum. *J. Cell Biol.* **109,** 2045-2055.

Leterrier, J.-F., Linden, M. and Nelson, B. D. (1990) How do microtubules interact in vitro with purified subcellular organelles? *Biochem. J.* **269,** 556-558.

Lin, A., Krockmalnic, G. and Penman, S. (1990). Imaging cytoskeleton-mitochondrial membrane attachments by embedment-free electron microscopy of saponin-extracted cells. *Proc. Nat. Acad. Sci. USA.* **87,** 8565-8569.

Luzikov, V. N., Zubatov, A. S. and Rainina, E. I. (1973). Formation and degradation of mitochondria in the cell. *J. Bioenergetics* **5,** 129-149.

Luzikov, V. N., Zubatov, A. S., Rainina, E. I. and Bakeyeva, L. E. (1971). Degradation and restoration of mitochondria upon deaeration and subsequent aeration of aerobically grown Saccharomyces cerevisiae cells. *Biochim. Biophys. Acta* **245,** 321-334.

Magrassi, L., Purves, D. and Lichtman J.W. (1987). Fluorescent probes that stain living nerve terminals. *J. Neurosci.* **7,** 1207-1214.

Maness, P. F., Aubry, M., Shores, C. G., Frame, L. and Pfenninger, K. H. (1988). *c-src* gene product in developing rat brain is enriched in nerve growth cone membranes. *Proc. Nat. Acad. Sci. USA* **85,** 5001-5005.

Mattson, M. P., Taylor-Hunter, A. and Kater, S. B. (1988). Neurite outgrowth in individual neurons of a neuronal population is differentially regulated by calcium and cAMP. *J. Neurosci.* **8,** 1704-1711.

Martz, D., Lasek, R. J., Brady, S. T. and Allen, R. D. (1984). Mitochondrial motility in axons: membranous organelles may interact with the force generating system through multiple surface binding sites. *Cell Motil.* **4,** 89-101.

McLean, I. W. and Nakane, P. K. (1974). Periodate-lysine-paraformaldehyde fixative: a new fixative for immunoelectron microscopy. *J. Histochem. Cytochem.* **22,** 1077-1083.

Miller, R. H. and Lasek, R. J. (1985). Cross-bridges mediate anterograde and retrograde vesicle transport along microtubules in squid axoplasm. *J. Cell Biol.* **101,** 2181-2193.

Paschal, B. M., Shpetner, H. S. and Vallee, R. B. (1987). MAP 1C is a microtubule-activated ATP-ase which translocates microtubules in vitro and has dynein-like properties. *J. Cell Biol.* **105,** 1273-1282.

Porter, M. E., Scholey, J. M., Stemple, D. L., Vigers, G. P., Vale, R. D., Sheetz, M. P. and McIntosh, J. R. (1987). Characterization of the microtubule movement produced by sea urchin egg kinesin. *J. Biol. Chem.* **262,** 2794-2802.

Price, M. G. and Gomer, R. H. (1989). Mitoskelin: a mitochondrial protein found in cytoskeletal preparations. *Cell Motil.* **13,** 274-287.

Rehder, V. and Kater, S. B. (1992). Regulation of neuronal growth cone filopodia by intracellular calcium. *J. Neurosci.* **12,** 3175-3186.

Reinsch, S. S., Mitchison, T. J. and Kirschner, M. (1991). Microtubule polymer assembly and transport during axonal elongation. *J. Cell Biol.* **115,** 365-379.

Rendon, A., Jung, D. and Jancsik, V. (1990). Interaction of microtubules and microtubule-associated proteins (MAPs) with rat brain mitochondria. *Biochem. J.* **269,** 555-556.

Sahenk, Z. and Brown, A. (1991). Weak-base amines inhibit the anterograde-to-retrograde conversion of axonally transported vesicles in nerve terminals. *J. Neurocytol.* **20,** 365-375.

Sahenk, Z. and Lasek, R. J. (1988). Inhibition of proteolysis blocks anterograde-retrograde conversion of axonally transported vesicles. *Brain Res.* **460,** 199-203.

Sato-Yoshitake, R., Yorifuji, H., Inagaki, M. and Hirokawa, N. (1991). Phosphorylation of kinesin regulates its binding to synaptic vesicles. *J. Cell Biol.* **115,** 390a. (abstr).

Sawin, K. E., Mitchison, T. J. and Wordeman, L. G. (1992). Evidence for kinesin-related proteins in the mitotic apparatus using peptide antibodies. *J. Cell Sci.* **101,** 303-313.

Saxton, W. M., Porter, M. E., Cohn, S. A., Scholey, J. M., Raff, E. C. and McIntosh, J. R. (1988). Drosophila kinesin: characterization of microtubule motility and ATPase. *Proc. Nat. Acad. Sci. USA* **85,** 1109-1113.

Schnapp, B. and Reese, T.S. (1982). Cytoplasmic structure in rapid-frozen axons. *J. Cell Biol.* **94,** 667-679.

Schnapp, B. and Reese, T.S. (1989). Dynein is the motor for retrograde axonal transport of organelles. *Proc. Nat. Acad. Sci. USA* **86,** 1548-1552.

Schroer, T. A. and Sheetz, M. P. (1991). Functions of microtubule-based motors. *Annu. Rev. Physiol.* **53,** 629-652.

Schroer, T. A., Steuer, E. R. and Sheetz, M. P. (1989). Cytoplasmic dynein is a minus end-directed motor for membranous organelles. *Cell* **56,** 937-946.

Smith, R. S. (1988). Studies on the mechanism of the reversal of rapid organelle transport in myelinated axons of *Xenopus laevis. Cell Motil.* **10,** 296-308.

Smith, R. S. and Snyder, R. E. (1991). Reversal of rapid axonal transport at a lesion: leupeptin inhibits reversed protein transport, but does not inhibit reversed organelle transport. *Brain Res.* **552,** 215-227.

Stromer, M. H. and Bendayan, M. (1990) Immunocytochemical identification of cytoskeletal linkages to smooth muscle cell nuclei and mitochondria. *Cell Motil.* **17,** 11-18.

Summerhayes, I. C., Wong, D. and Chen, L. B. (1983). Effect of microtubules and intermediate filaments on mitochondrial distribution. *J. Cell Sci.* **61,** 87-105.

Takenaka, T., Kawakami, T., Hikawa, N. and Gotoh, H. (1990). Axoplasmic transport of mitochondria in cultured dorsal root ganglion cells. *Brain Res.* **528,** 285-290.

Toyoshima, I., Yu, H., Steuer, E. R. and Sheetz, M. P. (1992). Kinectin, a major kinesin-binding protein on ER. *J. Cell Biol.* **118,** 1121-1132.

Tsukita, S. and Ishikawa, H. (1980). The movement of membranous organelles in axons. *J. Cell Biol.* **84,** 513-30.

Vale, R. D., Reese, T. S. and Sheetz, M. P. (1985a). Identification of a novel force-generating protein, kinesin, involved in microtubule-based motility. *Cell* **42,** 39-50.

Vale, R. D., Schnapp, B. J., Mitchison, T., Steuer, E., Reese, T. S. and

Sheetz, M. P. (1985b). Different axoplasmic proteins generate movement in opposite directions along microtubules in vitro. *Cell* **43,** 623-632.

Vallee, R. B. and Bloom, G. S. (1991). Mechanisms of fast and slow axonal transport. *Annu. Rev. Neurosci.* **14,** 59-92.

Van Blerkom, J. (1991). Microtubule mediation of cytoplasmic and nuclear maturation during the early stages of resumed meiosis in cultured mouse oocytes. *Proc. Nat. Acad. Sci. USA* **88,** 5031-5035.

Zielinski, B. S., Getchell, M. L. and Getchell, T. V. (1988). Ultrastructural characteristics of sustentacular cells in control and odorant-treated olfactory mucosae of the salamander. *Anat. Rec.* **221,** 769-779

.

(Received 15 October 1992 - Accepted 2 December 1992)